JOURNAL OF PETROLEUM GEOMECHANICS
(JPG)

Original article

3D Numerical modeling of the effect of in-situ stress ratio on mud weight window in the drilling of the Zagros sedimentary basin

Mohammad Reza Aghakhani Emamqeysi [1], Mohammad Fatehi Marji [1*], Abbas Hashemizadeh [2], Manouchehr Sanei [1], Abolfazl Abdollahipour [3]

1- Mine Exploitation Engineering Department, Faculty of Mining and Metallurgy, Institutive of Engineering, Yazd University, Yazd, Iran
2- Petroleum Engineering Department, Petroleum and Petrochemical Engineering School, Hakim Sabzevari University, Sabzevar, Iran.
3- School of Mining Engineering, College of Engineering, University of Tehran, Tehran, Iran

Received: 30 June 2022 ; Accepted: 13 September 2022

DOI: 10.22107/jpg.2022.349740.1172

Keywords

Geomechanical model,
Wellbore stability,
In-situ stress,
Mohr-Coulomb,
Mogi-coulomb

Abstract

The study of factors affecting wellbore stability has become very important in the oil and gas industry because they will save time and costs. In studying the stability of oil and gas wells, different factors such as mechanical properties, in-situ stresses, and pore pressure can be used. Consequently, knowing and calculating these parameters will be helpful in analyzing the wellbore stability. This study evaluated the effects of changing stresses on the wellbore stability and drilling mud weight window using a ratio of different stresses for the first time in one of the wells of the Zireh gas field, located in the southwest of Iran. Due to the lack of laboratory data, each of the parameters of the geomechanical model were determined by empirical correlation. Using Mohr-Coulomb and Mogi-Coulomb criteria, the drilling mud weight window was determined to be 76.99-128.17 (pcf) and 67.56-128.17 (pcf), respectively; however, Mogi-Coulomb provided better results. The wellbore stability is also investigated by using 3D numerical modeling using ABAQUS software and the Mohr-Coulomb criterion. According to the results of the numerical and analytical methods, the well is completely stable. Ultimately, five different in-situ stress ratios were examined to determine how in-situ stress distribution affected wellbore stability. According to the results, the mud weight window range decreases as the stress changes from an isotropic to an anisotropic state, indicating wellbore instability.

1. Introduction

In recent years, geomechanics has been introduced as an important and essential knowledge in exploration, development, production and operation of oil and gas companies in the world. The tasks of geomechanics include studying and analyzing the behavior of the earth against stresses, fluid pressures and temperature changes. The wellbore stability is a topic extensively researched in geomechanics. so, by analyzing the wellbore stability beforehand can prevent a great deal of basic problems, such as the collapse and fractures in the well. These instabilities can lead to problems such as stuck pipes, breakouts, tensile and compressive cracks in the well, and mud loss [1]. Due to these cases, the time and costs of drilling operations can be significantly reduced by recognizing and reacting to wellbore instabilities before the drilling operations take place. The first step in studying wellbore stability is to create a geomechanical model. Geomechanical models can be created by using geological, petrophysical, and geophysical information on the study area. Mechanical properties such as Young's modulus, Poisson's ratio, bulk modulus, shear modulus, uniaxial compressive strength, tensile strength, friction angle and cohesion, as well as in-situ stresses and pore pressure will be calculated to construct the geomechanical model. After determining these

* Yazd, Yazd University, Faculty of Mining and Metallurgy, TEL: 03531232593, Email: mfatehi@yazd.ac.ir; mohammad.fatehi@gmail.com

parameters, the final step is to determine the optimal mud weight window. Aadnoy & Chenevert [2], Brody & Kjorholt [3] as well as. Zoback et al. [4] have proposed various methods, including determining in-situ stresses in deep horizontal and vertical wells, the use of FMI logs, and the use of solid mechanics, to analyze the stability of highly inclined wells. Also, using failure criteria is one of the steps of wellbore stability analysis. Vernik & [5], Zhou [6], Song & Haimson [7], Ewy [8], Fjar & Ruistuen [9] and Al-Ajmi & Zimmerman [10] have used various failure criteria including Mohr-Coulomb, modified lade and Mogi-Coulomb to analyze wellbore stability. Das & Chatterjee used three Mohr-Coulomb, Mogi-Coulomb and modified lade criteria to analyze wellbore stability. The Mohr-Coulomb failure criteria exceeded the predicted mud weight window, but the Mogi-Coulomb criterion approximated the results with high accuracy close to the expected results [11]. Najibi et al. the mud weight window was determined by using the Mohr-Coulomb and Mogi-Coulomb failure criteria using data from one of the Bangestan reservoir wells. The accuracy of the geomechanical model based on the FMS log was then evaluated [12]. Yousefian et al. examined the plastic area around vertical wells using elastoplastic analysis and Mohr-Coulomb, Mogi-Coulomb, and modified Lade failure criteria. The results showed that the criterion Mogi-Coulomb and the modified lade did not show any plastic area around the well, which was in good agreement with the FMI log results [13]. Behnam et al. used FLAC^{2D} software and the NYZA method to calculate the minimum drilling mud pressure required to prevent shear failure. Finally, SPSS software was used to obtain correlation through multivariate linear regression [14]. Ezati et al. have analyzed wellbore stability using data from Sarvak reservoir in southwest Iran. The mechanical and strength parameters of the formation were determined with rock mechanics tests and wellbore stability was evaluated with Mohr-Coulomb and Mogi-Coulomb failure criteria. The results demonstrated that the Mogi-Coulomb criterion was more accurate in predicting well failure [15]. Allawi & Al-Jawad used the Mohr-Coulomb, Mogi-Coulomb, and modified Lade criteria to determine the drilling mud weight window of the Zubair Shale formation in southern Iraq. Ultimately, it was determined that improper selection of drilling mud weight is the primary cause of instability in this formation, and the appropriate mud weight window for drilling in this formation was calculated [16]. Hoseinpour & Riahi using the data of one of Iran's hydrocarbon reservoirs and using geomechanical parameters to determine the drilling mud weight window, select the appropriate drilling direction and study the wellbore stability [17]. Heydari et al. use data from the Sivand oil field to investigate the problem of wellbore stability analysis and optimal drilling direction using numerical modelling based on finite element method, and to determine safe mud weight windows using NYZA method [18].

Many studies have been conducted on wellbore stability and drilling mud weight window using numerical and analytical methods. However, analysis of in-situ stresses have not been discussed much despite their impact on drilling mud weight window ranges. Thus, this study attempts to determine the drilling mud weight window range by developing a geomechanical model, and finally, effect of changing the ratio of in-situ stresses on drilling mud weight window and wellbore stability was studied using three-dimensional numerical modeling. The new innovation in this study was the use of new equations between dynamic and static elastic parameters for carbonate rocks, followed by the development of 1D geomechanical models and 3D numerical models for wellbore stability analysis. The following steps have been done to achieve the research purpose. First, using petrophysical data such as compressive and shear wave transmit time, compressive and shear wave velocity, density and porosity, a geomechanical model of the reservoir was constructed. Then, using mechanical parameters, in-situ stresses, as well as pore pressure, drilling mud weight window were calculated for one of the wells in southwest Iran. The upper and lower limits of the mud weight window were determined using Mohr-Coulomb and Mogi-Coulomb failure criteria. Finally, using a three-dimensional elastoplastic finite element model, the analytical method was validated and the effects of different in-situ stresses on wellbore stability and drilling mud weight window ranges were examined.

2. Geological Setting

Zireh gas field is located 160 km southeast of

Bushehr near the Kangan and Nar gas fields. Field dimensions are 16×45 km, and it is located in a northwest-southeast direction. Also, its southeast direction faces Nar field, and its northwest direction faces Shir field. This study focuses on the Zireh well-2. The well is located near axis of Zireh anticline and approximately 2 km southeast of anticline peak. The coordinates of the well are E52 00 24, N 28 06 27. According to petrophysical studies and drilling reports, the sequence of the main formations in the study area is Kazhdumi, Darian, Fahliyan, Kangan, Dalan, Nar, and lower Dalan. As shown in Fig. 1, the gas reservoir in this study is located in the lower Dalan formation. Petrophysical studies indicate that lower Dalan rocks are mainly composed of carbonate rocks, including dolomite, anhydrite, and iron ores including siderite, hematite, and magnetite.

In this study, the parameters used to determine the geomechanical model is sonic, density, and caliper logs for depth intervals of 2650 to 2820 meters, and these parameters are given in Fig. 2.

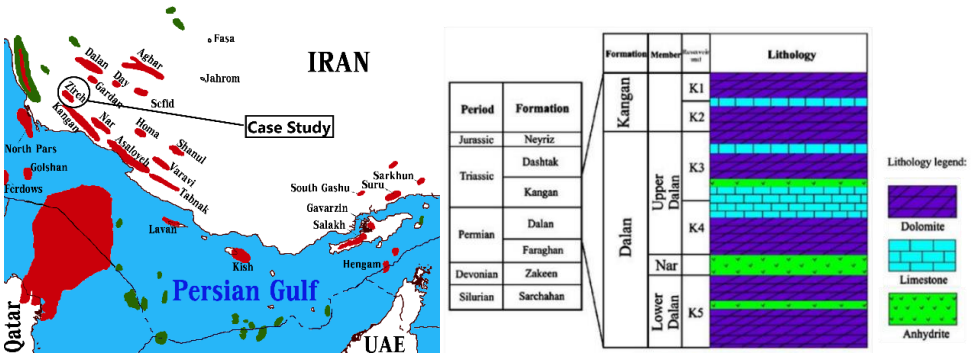

Fig. 1. Location and stratigraphic column of Zireh gas field, SW Iran [19]

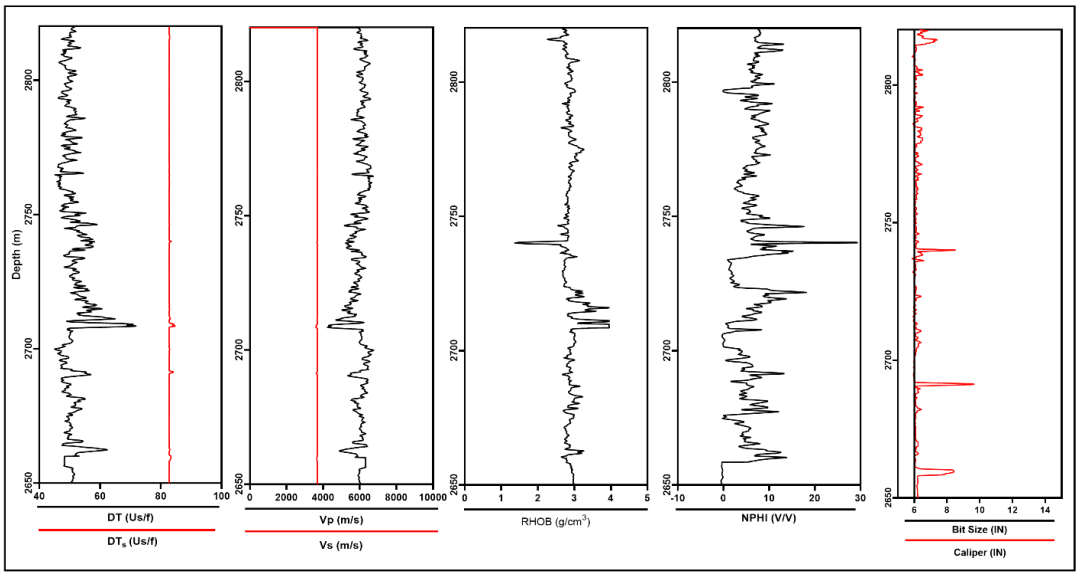

Fig. 2. Density (RHOB), porosity (NPHI), V_p and V_s, DT and DT_s logs for the Zireh gas reservoir in the study well

3. Geomechanical modeling

3.1 Mechanical properties

Throughout the life of an oil and gas field, it is essential to know the mechanical properties of the rock, such as Young's modulus, Poisson's ratio, uniaxial compressive strength, shear modulus, and bulk modulus. Elastic properties can be determined using two different methods. The first involves laboratory tests in which the properties of strength and elastic can be determined using

core samples. In the second method, measurements from in-well are used, in which the compressive and shear wave velocities are measured, which are called static and dynamic moduli, respectively. Uniaxial or triaxial loads will cause failure within the rock sample in the static method. During the test, stresses as well as lateral and axial deformations of the rock will be continuously measured by using the strain and stress data from the uniaxial compressive strength (UCS), static Young's modulus (E_s), and Poisson's ratio (ϑ).

The dynamic method uses field data (sonic logs) or laboratory measurements to determine the compressive and shear wave velocities (V_p and V_s) for rock samples affected by wave propagation loads. Based on density and sonic log data, the parameters are determined as follows [20].

$$E_d = \rho\, V_s^2\, \frac{3V_p^2 - 4V_s^2}{V_p^2 - V_s^2} \quad (1)$$

$$\vartheta_d = \frac{V_p^2 - 2V_s^2}{2(V_p^2 - V_s^2)} \quad (2)$$

$$K_d = \rho V_p^2 - \frac{4}{3}\rho V_s^2 \quad (3)$$

$$G_d = \rho\, V_s^2 \quad (4)$$

where E_d is the dynamic Young's modulus (GPa), ρ is rock density (g/cm^3), V_s is shear wave velocity in (km/s), V_p is compressive wave velocity (km/s), ϑ_d is dynamic Poisson's ratio, K_d is dynamic bulk modulus and G_d is dynamic shear modulus (GPa).

Given the continuity of data obtained using dynamic method, static and dynamic moduli are combined or dynamic data is transformed into static data in order to improve accuracy and achieve certainty in calculations. As a result, the problem of dynamic data discretization during calculation is eliminated, as are any uncertainty in the dynamic data while at the same time achieving a reliable approximation of the elastic properties of the well at any desired depth. Several equations between dynamic and static parameters have been developed to calculate the static elastic parameters. These equations are dependent on the material of formation and the study area. Due to the carbonate rock in this study, Eqs. 5 and 6 can be used to determine the static Young's modulus and static Poisson's ratio. Additionally, equations based on Young's modulus and Poisson's ratio have been developed to calculate bulk modulus and shear modulus (Eqs.7 and 8) [21].

$$E_s = 0.5624\, E_d - 13.91 \quad (5)$$

$$\vartheta_s = 0.72\, \vartheta_d \quad (6)$$

$$G_s = \frac{E_s}{2(1+\vartheta_s)} \quad (7)$$

$$K_s = \frac{E_s}{3(1-2\vartheta_s)} \quad (8)$$

The next parameter to consider in geomechanical modeling is the uniaxial compressive strength (UCS). This parameter is obtained by two methods including uniaxial and triaxial tests on core samples and using different empirical correlations presented by different researchers. Seyedsajadi & Aghighi [22] have derived an empirical correlation (Eq. 9) between compressive strength and Young's modulus parameters on carbonate rock cores from the Koopal field using the results of laboratory tests. Furthermore, the correlation coefficient related to this relationship is 0.98, indicating the accuracy of this equation for calculating uniaxial compressive strength. The uniaxial tensile strength is another parameter that can be determined as a coefficient of UCS based on the type of formation. As the formation is a carbonate, Eq. 10 will be used to determine the tensile strength.

$$UCS = 1.192\, E_s + 6.787 \quad (9)$$

$$T_0 = \frac{UCS}{12} \quad (10)$$

Friction angle and cohesion are two other mechanical parameters intrinsic to rocks. These parameters are also obtained using triaxial test as well as empirical correlations. Since laboratory tests were not available in this study, Eqs.11 and 12, which are presented for friction angle and cohesion based on porosity and shale volume, respectively [12].

$$\varphi = 26.5 - 37.4(1 - NPHI - V_{shale}) + 62.1(1 - NPHI - V_{shale})^2 \quad (11)$$

$$c = \frac{UCS}{2\tan\theta} \quad (12)$$

where φ is friction angle (degree), c is cohesion (MPa), NPHI is porosity, UCS is uniaxial compressive strength (MPa) and V_{shale} is

shale volume. The parameters of shale volume and θ are calculated using Eqs. 13 and 14 [23,24].

$$V_{shale} = \frac{GR - GR_{min}}{GR_{max} - GR_{min}} \quad (13)$$

$$\theta = 45 + \frac{\varphi}{2} \quad (14)$$

where GR is gamma ray (API).

3.2 Pore Pressure

One of the most important parameters in the construction of a geomechanical model is the pore pressure, which can be used to calculate in-situ stresses, analyze wellbore stability, and design a safe drilling mud weight window. In general, direct measurement methods, such as DST, RFT, MDT, as well as using geophysical logs and seismic data can be used to determine pore pressure. Also, if the pore pressure is calculated from indirect methods, it should be calibrated using direct measurement methods to ensure the result obtained.

Many researchers have proposed empirical equations for calculating pore pressure [25-27]. Eaton [28] is one of the most widely used methods for calculating the pore pressure. Using resistivity or sonic log data, pore pressure is calculated as follows:

$$P_{pg} = OBG - (OBG - P_{pn})\left(\frac{NCT}{DT}\right)^3 \quad (15)$$

where P_{PG} is pore pressure gradient, OBG is overburden gradient, P_{PN} is hydrostatic pressure gradient, DT is compressional wave transit time and NCT is normal compression trend line, which varies for different diagrams. Zhang [29] modified Eaton's equation (Eq. 15) and proposed Eq. 16 to predict pore pressure.

$$P_{pg} = OBG - (OBG - P_{pn})\left(\frac{\Delta t_m + (\Delta t_{ml} - \Delta t_m)e^{-cZ}}{DT}\right)^3 \quad (16)$$

where Δt_{ml} is mud-line transit time, Δt_m is compressional wave transit time in shale with zero porosity, c is an empirical constant and Z is depth. Also, by studying carbonate reservoirs in Iran, the values of Δt_m, Δt_{ml} and c have been estimated as 185, 50 and 0.00137, respectively [30].

3.3 In-situ Stresses

Overburden stress or vertical stress occurs due to the weight of layers of overburden in a formation. As it is not possible to calculate vertical stresses directly, it can be estimated by using the rock density at various depths and Eq. 17 as follows [31].

$$\sigma_v = \int_0^z \rho_b(z).g\,dz \quad (17)$$

where z is depth (m), $\rho_b(z)$ is density of the formation at different depths (g/cm^3), and g is acceleration of gravity.

There are many methods for calculating horizontal in-situ stresses, including LOT, XLOT, and hydraulic fracturing, which all rely on increasing the fluid pressure inside the well and creating a crack in the well wall. In order to calculate horizontal stresses using these tests, enough time, cost, and laboratory data are required. In addition, poroelastic equations are empirical equations derived from the calculation of horizontal stresses along the well, and were introduced as Eqs. 18 and 19 [20].

$$\sigma_h = \frac{\vartheta}{1-\vartheta}(\sigma_v - \alpha P_p) + \alpha P_p + \frac{E_s}{1-\vartheta^2}(\varepsilon_x + \vartheta\varepsilon_y) \quad (18)$$

$$\sigma_H = \frac{\vartheta}{1-\vartheta}(\sigma_v - \alpha P_p) + \alpha P_p + \frac{E_s}{1-\vartheta^2}(\varepsilon_y + \vartheta\varepsilon_x) \quad (19)$$

where σ_v is vertical stress (MPa), P_p is pore pressure (MPa), E_s is static Young's modulus (GPa), ϑ is Poisson's ratio, α is Biot's coefficient and ε_x , ε_y are strain in direction of maximum and minimum horizontal stresses as given by Eqs. 20 and 21, respectively [32].

$$\varepsilon_x = \frac{\sigma_v \times \vartheta}{E_s} \times \left(\frac{1}{1-\vartheta} - 1\right) \quad (20)$$

$$\varepsilon_y = \frac{\sigma_v \times \vartheta}{E_s} \times \left(1 - \frac{\vartheta^2}{1-\vartheta}\right) \quad (21)$$

3.4 Wellbore Stability

The final step in reservoir geomechanical modeling is to determine the mud weight window. This method necessitates designing and calculating an optimal mud pressure that prevents fractures, induced cracks, and wellbore instability. Fig. 3 shows a safe mud weight window between the pore pressure and S_3. In addition, there is also a mud weight window between breakout pressure and S_3, which is called a safe and stable interval and is the best case for drilling, since well failure and mud loss will be prevented [33].

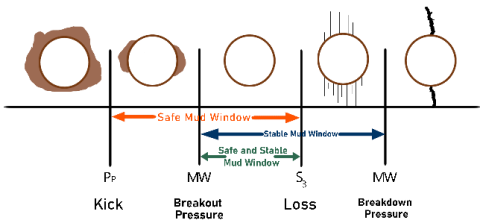

Fig. 3. A schematic of mud weight window intervals [18]

3.4.1 Stresses around a vertical wellbore

The drilling process disturbs the state of stress around the wellbore. The vertical stresses in a vertical well are parallel to the axis of the well, whereas the horizontal stresses are minimum and maximum perpendicular to each other. In a homogeneous, isotropic, elastic rock, the effective stresses around the well are calculated using Kirsch's equation (Eqs. 22-24) [33].

$$\sigma_\theta = \frac{1}{2}(\sigma_H - \sigma_h)\left(1+\frac{R^2}{r^2}\right) - \frac{1}{2}(\sigma_H - \sigma_h)\left(1+\frac{3R^4}{r^4}\right)\cos 2\theta - P_w\frac{R^2}{r^2} \quad (22)$$

$$\sigma_r = \frac{1}{2}(\sigma_H - \sigma_h)\left(1-\frac{R^2}{r^2}\right) + \frac{1}{2}(\sigma_H - \sigma_h)\left(1-\frac{4R^2}{r^2}+\frac{3R^4}{r^4}\right)\cos 2\theta - P_w\frac{R^2}{r^2} \quad (23)$$

$$\sigma_z = \sigma_v - 2\vartheta(\sigma_H - \sigma_h)\cos 2\theta \quad (24)$$

where r is distance from the well wall, R is well radius, P_w is well pressure, ϑ is Poisson's ratio and θ is measured clockwise from the σ_H direction. Also, these equations in the r = R will be simplified as follows:

$$\sigma_\theta = (\sigma_H + \sigma_h) - 2(\sigma_H - \sigma_h)\cos 2\theta - P_w \quad (25)$$

$$\sigma_r = P_w \quad (26)$$

$$\sigma_z = \sigma_v - 2\vartheta(\sigma_H - \sigma_h)\cos 2\theta \quad (27)$$

Tangential and radial stresses (Eqs. 25, 26) are affected by pore pressure, but axial stresses are not. Shear failure occurs at $\theta = \pm\pi/2$, where the tangential stress reaches its maximum value. Tensile failure occurs similarly at $\theta = 0, \pi$, where tangential stress is minimum.

3.4.2 Mohr-Coulomb failure criterion

This criterion is widely used due to the simplicity and availability of computational parameters such as uniaxial compressive strength and friction angle. Mohr-Coulomb criterion is calculated as follows [34].

$$\tau = S_0 + \sigma_n \tan\varphi \quad (28)$$

where S_0 is cohesion and φ is friction angle. In addition, equations for the Mohr-Coulomb criterion are presented based on maximum and minimum stresses, as shown in Eq. 29. As well as the parameter q, which is dependent on friction angle, and C_0 are shown in Eqs. 30 and 31 [10].

$$\sigma_1 = C_0 + q\sigma_3 \quad (29)$$

$$q = tan^2\left(45+\frac{\varphi}{2}\right) = \frac{1+\sin\varphi}{1-\sin\varphi} \quad (30)$$

$$C_0 = 2c\frac{\cos\varphi}{(1-\sin\varphi)} \quad (31)$$

Tables 1 and 2 give the collapse pressure and fracture pressure for the Mohr-Coulomb criterion. According to these tables, P_w is the actual drilling mud pressure, P_{wb} is the drilling mud pressure causing borehole failure, and P_{wf} is the drilling mud pressure causing fractures.

Table 1. Mohr–Coulomb criterion for collapse pressure in vertical wellbores [10]

Case	$\sigma_1 \geq \sigma_2 \geq \sigma_3$	Borehole failure will occur if $P_w \leq P_{wb}$
1	$\sigma_z \geq \sigma_\theta \geq \sigma_r$	$P_{wb} = (B-C)/q$
2	$\sigma_\theta \geq \sigma_z \geq \sigma_r$	$P_{wb} = (A-C)/(1+q)$
3	$\sigma_\theta \geq \sigma_r \geq \sigma_z$	$P_{wb} = A - C - qB$

$A = 3\sigma_H - \sigma_h$
$B = \sigma_v + 2\vartheta(\sigma_H - \sigma_h)$
$C = C_0 - P_p(q-1)$

Table 2. Mohr–Coulomb criterion for fracture pressure in vertical wellbores [10]

Case	$\sigma_1 \geq \sigma_2 \geq \sigma_3$	Borehole failure will occur if $P_w \geq P_{wf}$
1	$\sigma_r \geq \sigma_\theta \geq \sigma_z$	$P_{wf} = C + qE$
2	$\sigma_r \geq \sigma_z \geq \sigma_\theta$	$P_{wf} = (C+qD)/(1+q)$
3	$\sigma_z \geq \sigma_r \geq \sigma_\theta$	$P_{wb} = (C-E)/q + D$

$E = 3\sigma_h - \sigma_H$
$D = \sigma_v - 2\vartheta(\sigma_H - \sigma_h)$

3.4.3 Mogi-Coulomb failure criterion

Al-Ajmi & Zimmerman [10] first proposed the Mogi-Coulomb criterion. Although this criterion is more complex than the Mohr–Coulomb failure criterion, it has performed better in analyzing the results, so it has gained more acceptance recently. In addition, the equations for the Mogi-Coulomb

criterion are as follows [35].

$$\tau_{oct} = a + b\sigma_{m,2} \quad (32)$$

$$\tau_{oct} = \frac{1}{3}\sqrt{(\sigma_1 - \sigma_2)^2 + (\sigma_2 - \sigma_3)^2 + (\sigma_1 - \sigma_3)^2} \quad (33)$$

$$\sigma_{m,2} = \frac{\sigma_1 + \sigma_3}{2} \quad (34)$$

Parameters a and b are also material constants, which can be obtained by using the Mohr–Coulomb parameters of cohesion and friction angle. The equations for these parameters are given below [10].

$$a = \frac{2\sqrt{2}}{3} c \cos\varphi \quad (35)$$

$$b = \frac{2\sqrt{2}}{3} \sin\varphi \quad (36)$$

Eq. 37 is introduced as follows to calculate the primary and secondary stress constants (I_1 and I_2) by applying the main intermediate stress and modifying the Mogi-Coulomb equation [10].

$$I_1 = \sigma_1 + \sigma_2 + \sigma_3$$
$$I_2 = \sigma_1\sigma_2 + \sigma_2\sigma_3 + \sigma_3\sigma_1 \quad (37)$$

By considering the effective stress, Mogi-Coulomb criterion can be written as, [10].

$$(I_1^2 - 3I_2^2)^{1/2} = \acute{a} + \acute{b}(I_1 - \sigma_2 - 2P_0) \quad (38)$$

$$\acute{a} = 2c\ \cos\varphi \qquad \acute{b} = \sin\varphi \quad (39)$$

The collapse pressure and fracture pressure of the Mogi-Coulomb criterion are given in Tables 3 and 4.

Table 3. Mogi–Coulomb criterion for collapse pressure in vertical wellbores [10]

Case	$\sigma_1 \geq \sigma_2 \geq \sigma_3$	Borehole failure will occur if $P_w \leq P_{wb}$
1	$\sigma_z \geq \sigma_\theta \geq \sigma_r$	$P_{wb} = \frac{1}{6-2b'^2}\left[(3A + 2b'K) - \sqrt{H + 12(K^2 + b'AK)}\right]$
2	$\sigma_\theta \geq \sigma_z \geq \sigma_r$	$P_{wb} = \frac{A}{2} - \frac{1}{6}\sqrt{12[a' + b'(A - 2P_p)]^2 - 3(A - 2B)^2}$
3	$\sigma_\theta \geq \sigma_r \geq \sigma_z$	$P_{wb} = \frac{1}{6-2b'^2}\left[(3A - 2b'G) - \sqrt{H + 12(G^2 + b'AG)}\right]$

$A = 3\sigma_H - \sigma_h$
$B = \sigma_v + 2\vartheta(\sigma_H - \sigma_h)$
$K = a' + b'(B - 2P_p)$
$H = A^2(4b'^2 - 3) + (B^2 - AB)(4b'^2 - 12)$
$G = K + b'A$

Table 4. Mogi–Coulomb criterion for fracture pressure in vertical wellbores [10]

Case	$\sigma_1 \geq \sigma_2 \geq \sigma_3$	Borehole failure will occur if $P_w \geq P_{wf}$
1	$\sigma_r \geq \sigma_\theta \geq \sigma_z$	$P_{wf} = \frac{1}{6-2b'^2}\left[(3D + 2b'N) - \sqrt{J + 12(N^2 + b'DN)}\right]$
2	$\sigma_r \geq \sigma_z \geq \sigma_\theta$	$P_{wb} = \frac{D}{2} - \frac{1}{6}\sqrt{12[a' + b'(D - 2P_p)]^2 - 3(D - 2E)^2}$
3	$\sigma_z \geq \sigma_r \geq \sigma_\theta$	$P_{wb} = \frac{1}{6-2b'^2}\left[(3D - 2b'M) - \sqrt{J + 12(M^2 + b'DM)}\right]$

$E = 3\sigma_h - \sigma_H$
$D = \sigma_v - 2\vartheta(\sigma_H - \sigma_h)$
$N = a' + b'(E - 2P_p)$
$J = D^2(4b'^2 - 3) + (E^2 - DE)(4b'^2 - 12)$
$M = N + b'D$

4. Results and discussion

4.1 Geomechanical Modeling

Mechanical properties of rock such as Young's modulus, Poisson's ratio, shear modulus, bulk modulus, UCS, tensile strength, cohesion, and friction angle are among the parameters in determining in-situ stresses and also in wellbore stability analysis. For Zireh well-2, these parameters are calculated using Eqs. 1 - 14 for each parameter in the reservoir depth of 2650-2820 and are shown in Figs. 4 and 5 for elastic and strength parameters, respectively. The next parameter in creating the geomechanical model is the pore pressure. In this study, Eaton equation

(Eq. 16) was used to determine the pore pressure in this well, which is shown in Fig. 6.

In-situ stress values are among the critical parameters in reservoir geomechanical modeling. The vertical stress in well-2 is calculated based on Eq. 17 (shown in Fig. 6). Additionally, the poroelastic equations (Eqs. 18 and 19) along the well will be used to calculate the values of σ_H and σ_h. Fig. 6 shows that in most places, σ_H is approximately equal to σ_v, and both of them are larger than σ_h. Therefore, the stress regime in this depth is strike-slip normal ($\sigma_H = \sigma_v > \sigma_h$).

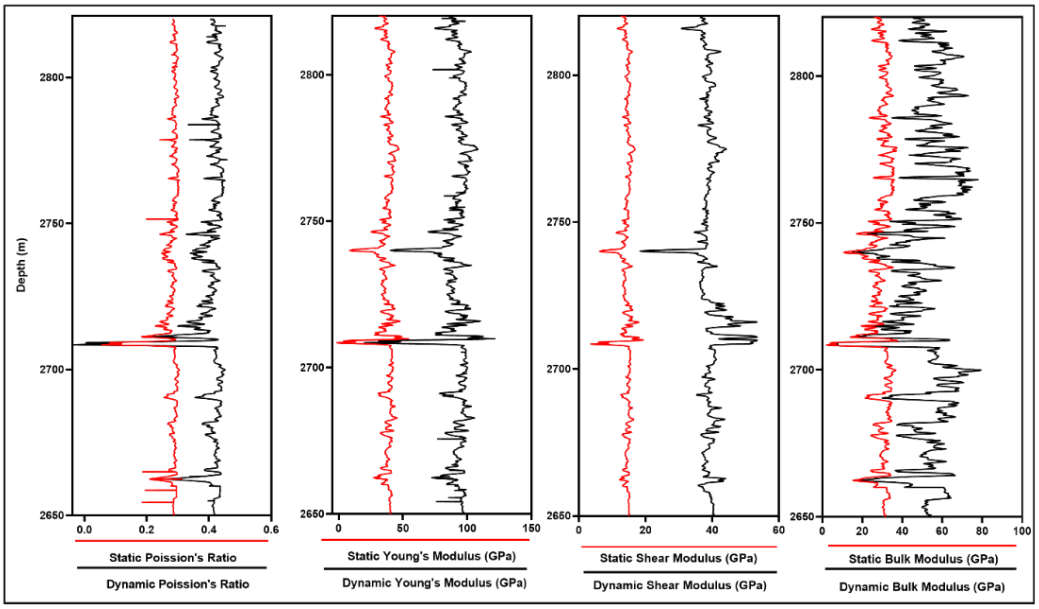

Fig 4. Static and dynamic elastic parameters of well-2 of the Zireh gas field at depths between 2650 and 2820

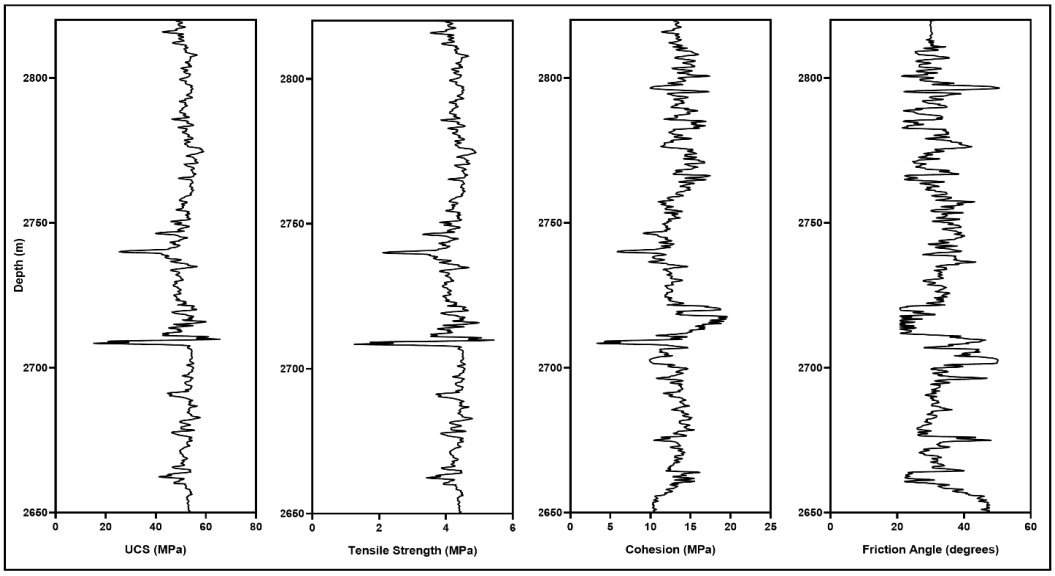

Fig. 5. Strength parameters of well-2 of the Zireh gas field at depths between 2650 and 2820

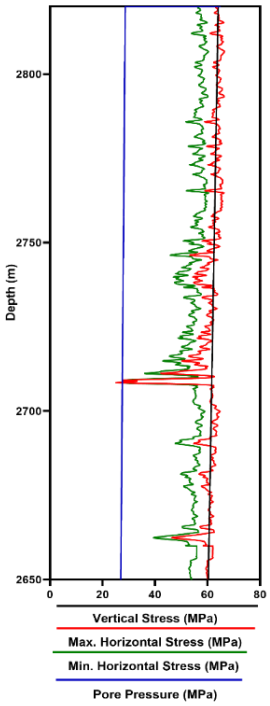

Fig. 6. σ_v, σ_H, σ_h and pore pressure of well-2 of the Zireh gas field at depths between 2650 and 2820

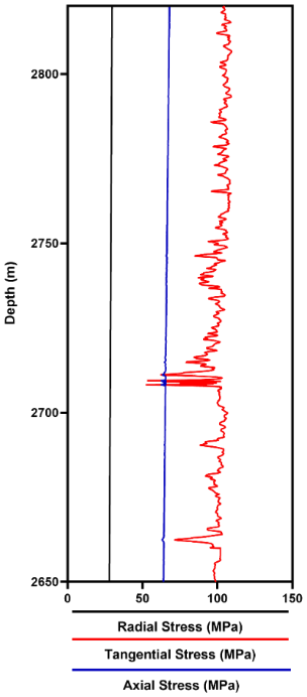

Fig. 7. Radial, tangential and axial stresses in the wall of well-2 of the Zireh gas field at depths between 2650 and 2820

4.2 Wellbore stability analysis

According to Fig. 7, the stresses around the well wall are $\sigma_\theta \geq \sigma_z \geq \sigma_r$, so the second equation in Tables 1 and 3 will be used to calculate the collapse pressure. Also, since the purpose of this study is to calculate the stable and safe mud weight window, the values of mud loss, which is equal to the minimum horizontal stress, were used for the upper limit of mud pressure. Finally, after calculating the mud pressure values for Mohr–Coulomb and Mogi-Coulomb criteria, these values are compared with the reported mud pressure values and if the Mohr–Coulomb and Mogi-Coulomb pressure values are higher than the mud pressure values, it will be cause shear fracture. In addition, if the mud pressure increases and reaches the values of mud loss (minimum horizontal stress), it will cause tensile fractures and wellbore instability.

In Fig. 8, the results of the Mohr-Coulomb and Mogi-Coulomb failure criteria are presented along with a caliper log for validation. In this figure, from left to right, the first column is related to wellbore stability analysis using Mohr-Coulomb, wellbore stability analysis using Mogi-Coulomb and caliper-bit size log results, respectively. Mohr-Columb criteria results are conservative in most parts, and comparing them to caliper logs can be seen that they have not provided accurate predictions in the areas where fracture caliper logs occur. The results obtained by the Mogi-Coulomb criteria indicate that this method has determined shear and tensile fractures with a higher accuracy. Comparison of the results from these two methods revealed that the Mogi-Coulomb criterion is more accurate than the Mohr-Coulomb criterion and is more reliable for predicting well fractures. To verify the accuracy of the results obtained by these failure criteria, the results obtained by well-2 of Zireh were compared to petrophysical evaluation reports for depths between 2660 and 2813 and the results showed there was no fall except for 2720 and 2691-2692. Other intervals are of good quality, which is well

suited to the results obtained in this study.

For Mohr-Coulomb and Mogi-Coulomb, the lower limit of the mud weight window is 76.99 pcf and 67.56 pcf, respectively, while the upper limit is 128.175 pcf (equivalent to the σ_h). According to the drilling reports of Zireh gas field for well-2, the value of 67 pcf for the drilling mud weight has been considered. According to the results obtained, Mohr-Coulomb criterion has more conservative results than Mogi-Coulomb because it does not use intermediate stress. Thus, the optimal mud weight window estimate generated using the Mogi-Coulomb criterion has higher accuracy than the Mohr-Coulomb criterion.

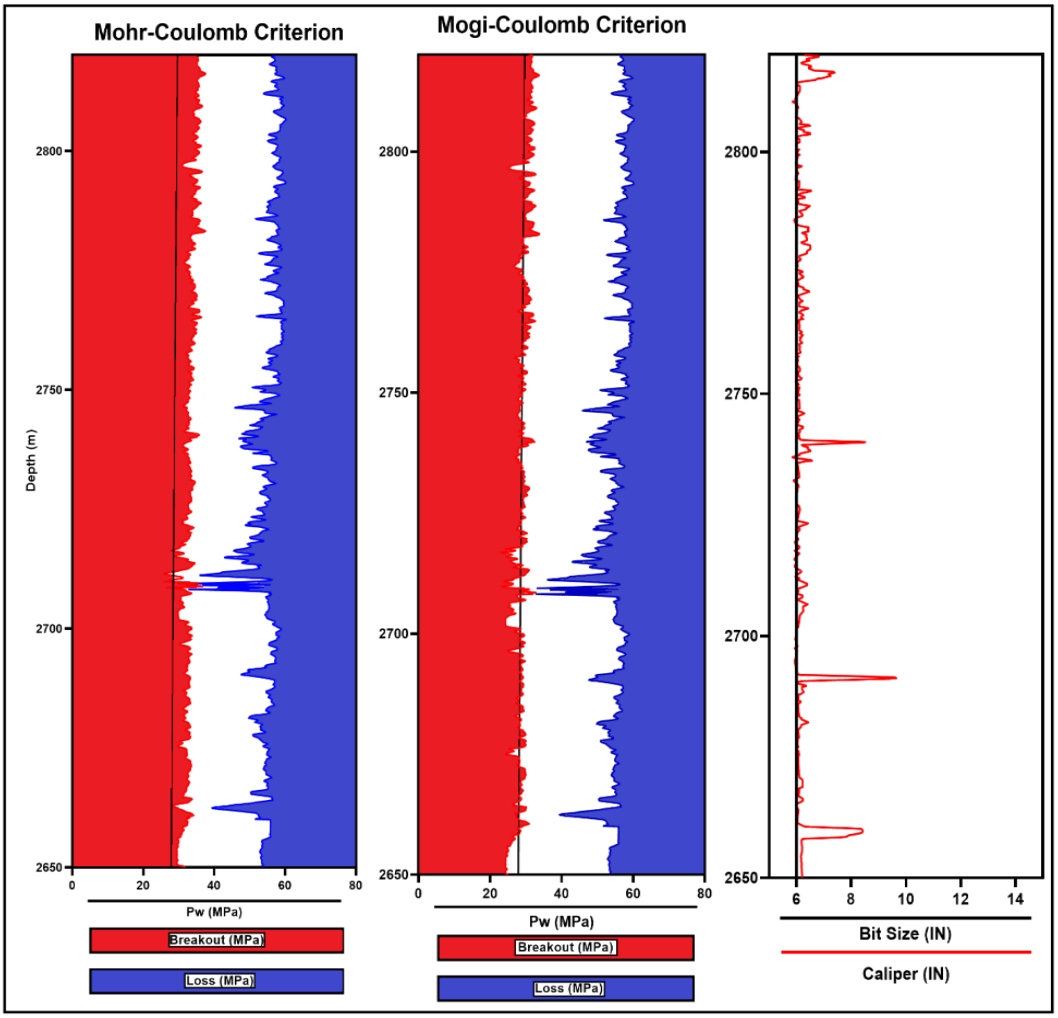

Fig.8. The wellbore stability analysis for well-2, in the depth interval of 2650 to 2820 m

4.3 Model validation

Finite element numerical method has been used to evaluate the accuracy of analytical methods calculations for drilling mud weight window. In this method, numerical methods are used to approximate the analysis and solution of partial differential equations. Using this method, differential equations are completely eliminated or reduced to ordinary differential equations [36]. ABAQUS software includes a library of finite elements that can be used to model any type of geometry. Also included is a large collection of material behavior models that simulate the behavior of metals, polymers, composites, reinforced concrete, brittle foams, and geotechnical materials such as soil and rock.

The 3D numerical model in this section was built for a critical section of the well with a depth range of 2720–2725 m. The first step in modeling is to determine the model's dimensions. According to drilling reports, the studied well has a diameter of 6 inches (0.1524 meters). In order to avoid the distribution of stresses around the well on the boundaries of the numerical model, the dimensions of the numerical model will be 100 times the radius of the well, as shown in Fig. 9. As a result of the double symmetry assumption, a quarter of the geometry is modeled to reduce analysis time. Behavioral model and material properties will then be created based on the Mohr-Coulomb criterion. The next step involves applying boundary conditions, in-situ stresses, and mud weight pressure to achieve equilibrium. Hydromechanical analysis can provide an acceptable approximation of the solution. In this case, the desired environment can be considered two-phase, meaning the space between solid particles is completely filled with liquid, which is called a saturated environment. In this study, the idea of effective stress was used to analyze saturated environments. Using this method, the effective stress was calculated by adding the pore pressure to the in-situ stresses. Numerical modelling relies heavily on meshing, so shape elements of hex and structured technique were used to mesh the 3D model. The geometry of the model will be divided into three parts, each with a different mesh size: 20×15 and 18×15 near the well wall and 15×15 near the model boundary. Based on the results, it is beneficial to use a finer mesh near the well in order to obtain more accurate results. The type of element used in this model is the plane strain.

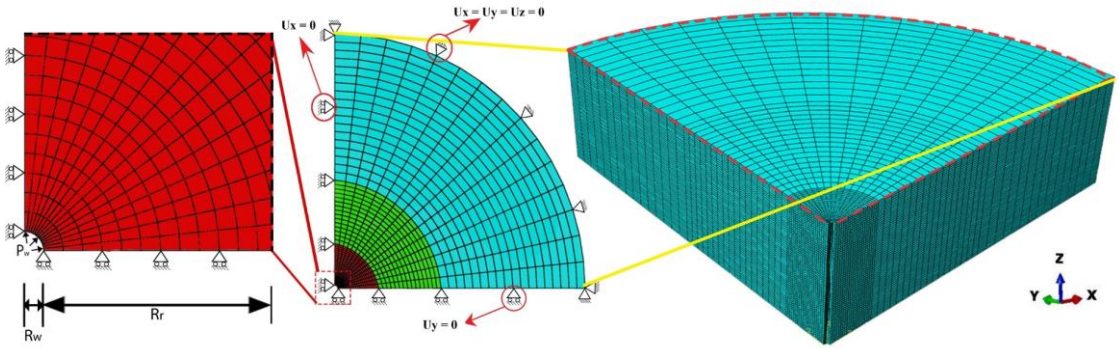

Fig. 9. The geometry of the model with boundary conditions and loading for wellbore stability analysis

Table 5. Input parameters for wellbore stability analysis in ABAQUS

Property		Value
Elastic	Specific weight (g/cm^3)	2.88
	Young's modulus (GPa)	37.340
	Poisson's ratio	0.28
Plastic	Cohesion (MPa)	13.25
	Internal friction angle (degree)	32.66
Strength	UCS (MPa)	51.29
	Tensile strength (MPa)	4.26
Fluid	Pore pressure (MPa)	27.83
	Mud pressure (MPa)	28.7
Petrophysical	Porosity (%)	17.2
	Permeability (md)	1.3
In-situ stresses	Vertical stress (MPa)	62.20
	Maximum horizontal stress (MPa)	61.44
	Minimum horizontal stress (MPa)	54.95

The results of the numerical model will be divided into two parts. The first part deals with the validity of wellbore stability as determined by the Mohr-Coulomb criterion analytical method, while the second part is about studying the effect of changing in-situ stresses on the drilling mud weight window. The mud weight window was validated by applying different pressures, in this case from 33 MPa to 54.95 MPa, obtained from the analytical method, and by examining the condition of the well at each pressure. Finally, the numerical model determined mud weight window range of 27.8 MPa to 48.2 MPa. Figs. 10 and 11 show the results of stress and displacement around the well. In addition, the results concerning the changes in plastic area were also obtained in this interval. Fig. 12 illustrates these results in addition to the analysis of the plastic area under 60 MPa pressure. For a better presentation of the results, using the mirror feature in the ABAQUS software, the results are shown around the well for all sides. Wellbore stability conditions are suitable as long as the expansion of the plastic area does not exceed the radius of the well. However, since the purpose of this study is to determine a safe and stable mud weight window, the beginning of the plastic area is regarded as instability.

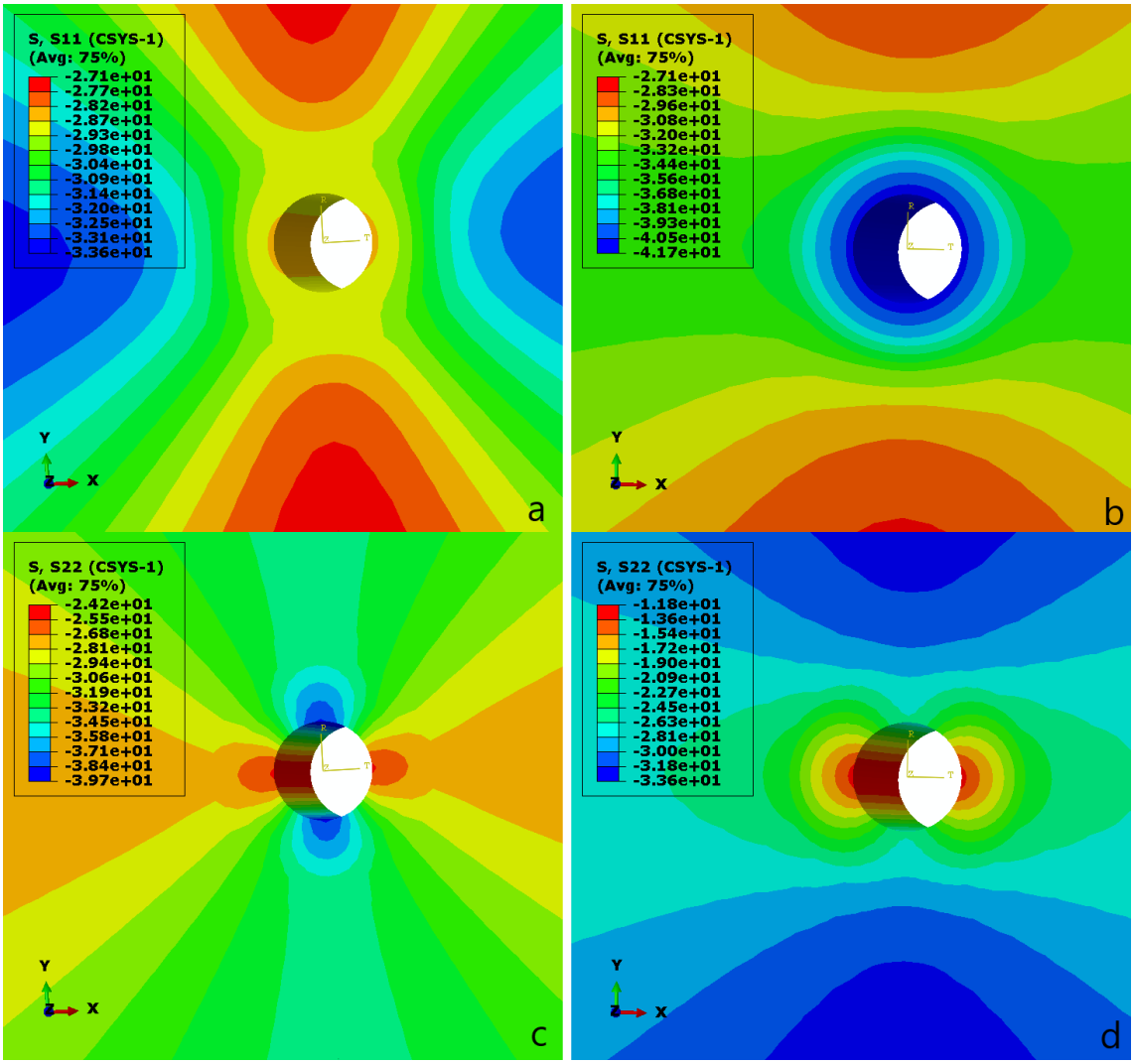

Fig. 10. Radial stress variations in the mud pressure, (a) 27.8 MPa, (b) 48.2 MPa, and tangential stress variations in the mud pressure, (c) 27.8 MPa, (d) 48.2 MPa

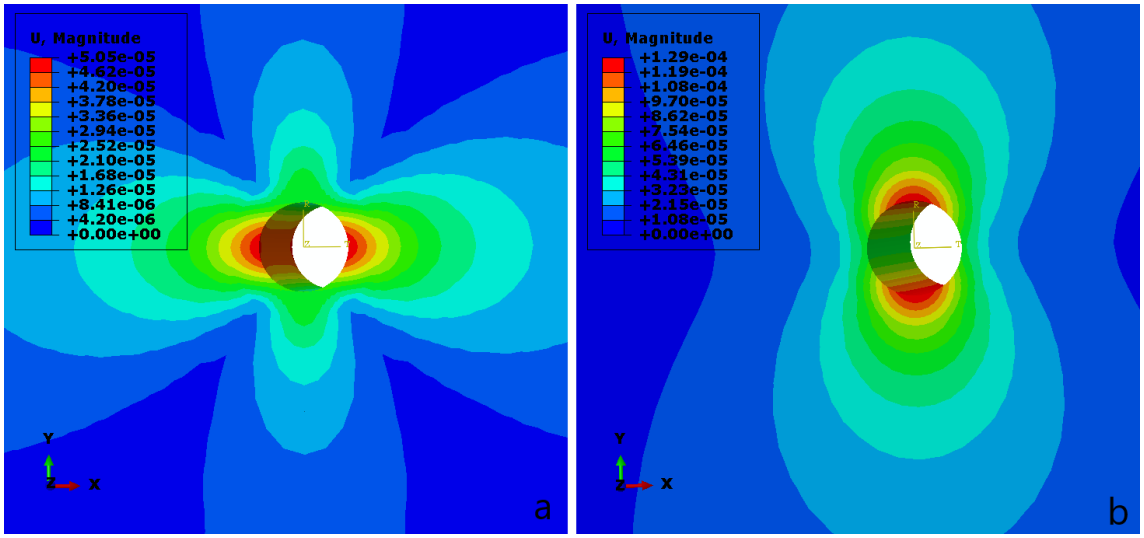

Fig. 11. Total deformation in the mud pressure, (a)27.8 MPa, (b) 48.2 MPa

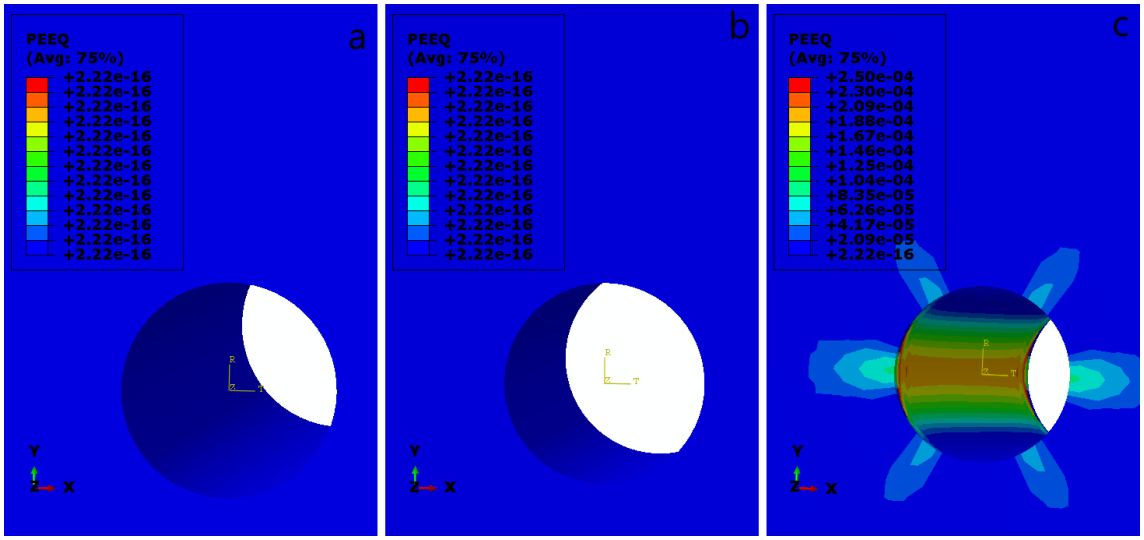

Fig. 12. Value of plastic strain for mud pressure, (a) 27.8 MPa, (b) 48.2 MPa, and (c) 60 MPa

Numerical analysis are used to calculate the probability of shear and tensile fractures in the well wall based on the strength characteristics of the study formation. Figs. 10, which are related to radial and tangential stresses. Due to in-situ stresses applied to the model and induction of such stresses along the formation boundary, maximum concentrations occur on the around well wall. According to Fig. 11, a circular deformation zone will form around the well if the applied stresses are isotropic. In this study, given that the horizontal in-situ stresses were anisotropic, the deformation zone around the well exhibited an ellipsoid extended. Also, Fig. 12 shows that there is no significant plastic area around the well in the mud weight window ranges, and the well is in an elastic state. Therefore, the considered well was identified as stable in the studied depth interval based on the results of the numerical analysis. The obtained results are in good agreement with the analytical results.

4.4 Effect of in-situ stress ratios

Studying the effectiveness of different parameters on wellbore stability facilitates a better comprehension of how these conditions impact wellbore stability. One of these parameters is in-situ stress. This section attempts to describe

results related to the plastic area and the changes to the mud pressure range by using data from the petrophysical studies and applying different scenarios for the ratio of in-situ stresses. The purpose of this section is to investigate the impact of different in-situ stress ratios on mud weight window. Table 6 shows the in-situ stress ratios for five different scenarios. The value of 1.24 in this table for the ratio of σ_H to σ_h indicates the in-situ stress regime (based on the geomechanical data from the Zireh well).

Table 6. Information about 5 different scenarios of in-situ stress ratio

Case	1	2	3	4	5
$\frac{\sigma_H}{\sigma_h}$	$\frac{\sigma_H}{\sigma_h} = 1$	$\frac{\sigma_H}{\sigma_h} = 1.24$	$\frac{\sigma_H}{\sigma_h} = 1.5$	$\frac{\sigma_H}{\sigma_h} = 1.75$	$\frac{\sigma_H}{\sigma_h} = 2$

In order to determine the effects of stress rate changes on wellbore stability, the σ_H and σ_h were varied using these scenarios and the appropriate mud weight window was obtained by applying different pressures to the well. Due to the fact that in the first two scenarios, the σ_H and σ_h are lower than the σ_v, the stress regimes are normal and no shear failures occur around the well, and the well is stable. In comparing these two scenarios, it can be concluded that the amount of drilling mud weight window range decreases when the stresses change from an isotropic to an anisotropic state. After examining the two in-situ stress ratios of 1.75 and 2, it was determined that in all the mud pressure that entered the well plastic zone was more severe with the stress ratio of 2 and mud weight window cannot be calculated for this stress ratio. As a result, mud pressure ranges are limited when the value of mud pressure changes from an isotropic to an anisotropic state until the amount of mud pressure is close to the mud weight window, causing wellbore instability. Considering the 5 stress ratio scenarios shown in Table 6, it is not possible to determine the exact point at which the mud weight window changed from stable to instable. By examining the stress ratios between 1.5 and 1.75, as shown in Fig.13, the exact value of the stress ratio that will cause wellbore instability was calculated.

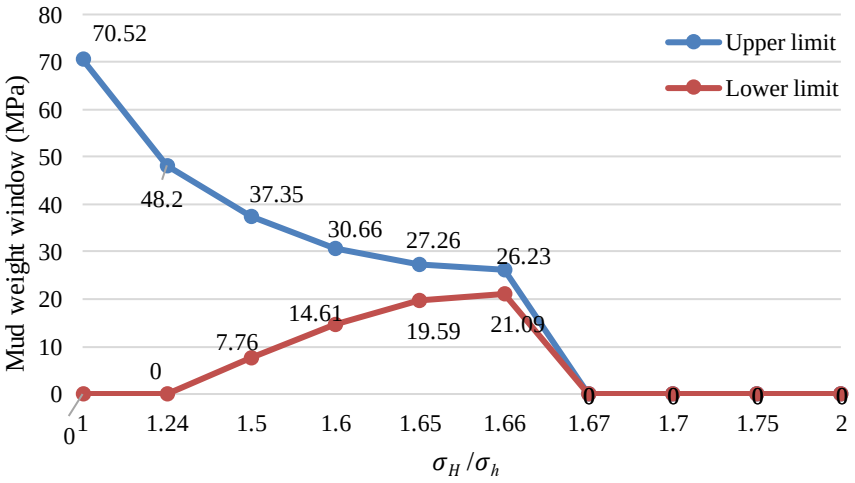

Fig. 13. Results of changing the mud weight window versus the in-situ stress ratios

In the first two cases (in-situ stress ratios 1 and 1.24) the lower limit value of mud pressure is zero, but as the in-situ stress ratio increases, more pressure is required, and the lower limit pressure increases. In addition, for the upper limit of mud pressure, with increasing the in-situ stress ratio, the mud weight window has been decreased to avoid tensile failure and mud loss. Finally, at a stress ratio of 1.66, the upper and lower limits will approach each other and cause instability. Shear

displacements and tensile fractures along the well are less observed when the stresses are assumed to be isotropic. When the rate of in-situ stress changes from isotropic to anisotropic, these fractures expand, allowing the drilling fluid to enter the fractures and increased mud loss eventually leads to wellbore instability. In Fig. 14, the plastic area for the two states of isotropic and anisotropic stresses is shown at a pressure of 27.8 MPa, which indicates the instability under anisotropic stress.

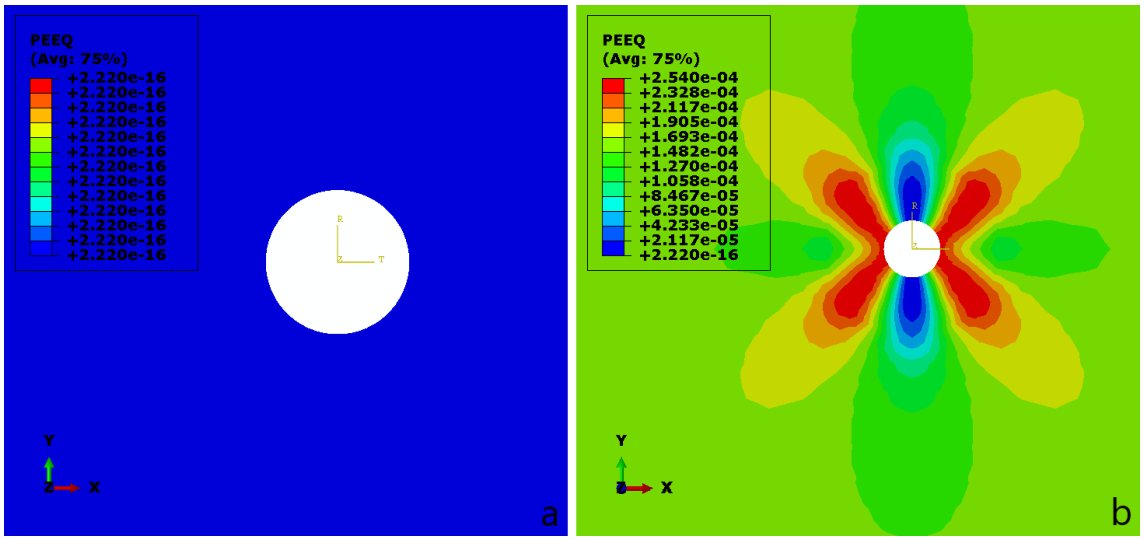

Fig. 14. The PEEQ for stress ratios of (a) isotropic ($\sigma_H/\sigma_h = 1$), (b) anisotropic ($\sigma_H/\sigma_h = 2$)

5. Conclusions

Wellbore instability is an issue that costs a lot of money each year. Understanding what causes it will aid in proper management of wells and will greatly reduce unnecessary expenses. The wellbore stability is considered to be of importance in this study, so an attempt was made to build a geomechanical model of the well and perform numerical and analytical analysis of the well using petrophysical data for the Zireh gas field. Also, the effects of changing in-situ stresses on mud weight window have been investigated, and the following results have been obtained as a result:

- The Mohr-Coulomb and Mogi-Coulomb criteria have been used to determine the safe and stable mud weight window. The comparison of these two methods revealed that because intermediate stresses do not have an effect on the Mohr-Coulomb failure criterion, the results of this criterion are conservative. In addition, comparing the Mogi-Coulomb criterion to the caliper log, it became apparent that this criterion is more accurate in predicting the mud weight window.
- Mohr-Coulomb and Mogi-Coulomb criteria specify a lower limit of mud weight window of 76.99 pcf and 67.56 pcf, respectively, and an upper limit of 128.17 pcf. According to the drilling reports of Zireh gas field for well-2, the value of 67 pcf for the drilling mud weight has been considered, which is close to the Mogi-Coulomb result.
- The Mohr-Coulomb criterion results were validated using the ABAQUS finite element, and mud weight window was obtained between 27.8 MPa and 48.2 MPa using the numerical method. Therefore, the numerical and analytical results were in good agreement.
- For the purpose of examining the effect of in-situ stress ratios on wellbore stability, five different in-situ stress ratios were considered. As a result, when the stress changes from isotropic to anisotropic, the mud weight window range is more limited, which indicates wellbore instability.
- In the anisotropic state, wellbore instability is caused by the occurrence of shear and tensile cracks around the well. Generally, the greater the ratio between the σ_H and σ_h, the more cracks

and mud loss will occur, which causes reduced mud pressure and wellbore instability.

6. References

[1] Al-Ajmi A. M., Zimmerman R. W. (2009). A new well path optimization model for increased mechanical borehole stability. Journal of Petroleum Science and Engineering;69(1-2):53-62.

[2] Aadnoy B., Chenevert M. (1987). Stability of highly inclined boreholes (includes associated papers 18596 and 18736). SPE Drilling Engineering;2(04):364-74.

[3] Brody M., Kjorholt H., editors. The initiation of drilling-induced tensile fractures and their use for the estimation of stress magnitude. Vail Rocks 1999, The 37th US Symposium on Rock Mechanics (USRMS); 1999: OnePetro.

[4] Zoback M., Barton C., Brudy M., Castillo D., Finkbeiner T., Grollimund B., et al. (2003). Determination of stress orientation and magnitude in deep wells. International Journal of Rock Mechanics and Mining Sciences;40(7-8):1049-76.

[5] Vernik L., Zoback M. D. (1992). Estimation of maximum horizontal principal stress magnitude from stress-induced well bore breakouts in the Cajon Pass scientific research borehole. Journal of Geophysical Research: Solid Earth;97(B4):5109-19.

[6] Zhou S. (1994). A program to model the initial shape and extent of borehole breakout. Computers & Geosciences;20(7-8):1143-60.

[7] Song I., Haimson B. C. (1997). Polyaxial strength criteria and their use in estimating in situ stress magnitudes from borehole breakout dimensions. International Journal of Rock Mechanics and Mining Sciences;34(3-4):116. e1-. e16.

[8] Ewy R. T. (1999). Wellbore-stability predictions by use of a modified Lade criterion. SPE Drilling & Completion;14(02):85-91.

[9] Fjar E., Ruistuen H. (2002). Chemistry and Physics of Minerals and Rocks/Volcanology-ECV 3-Impact of the intermediate principal stress on the strength of heterogeneous rock (DOI 10. 1029/2001 JB000277). Journal of Geophysical Research-Part B-Solid Earth;107(2):1.

[10] Al-Ajmi A. M., Zimmerman R. W. (2006). Stability analysis of vertical boreholes using the Mogi–Coulomb failure criterion. International Journal of Rock Mechanics and Mining Sciences;43(8):1200-11.

[11] Das B., Chatterjee R. (2017). Wellbore stability analysis and prediction of minimum mud weight for few wells in Krishna-Godavari Basin, India. International Journal of Rock Mechanics and Mining Sciences;93:30-7.

[12] Najibi A. R., Ghafoori M., Lashkaripour G. R., Asef M. R. (2017). Reservoir geomechanical modeling: In-situ stress, pore pressure, and mud design. Journal of Petroleum Science and Engineering;151:31-9.

[13] Yousefian H., Fatehi Marji M., Soltanian H., Abdollahipour A., Pourmazaheri Y. (2018). Stability analysis of a vertical wellbore in one of Iran's South-West oilfields using the plastic zone concept. Oil Geomechanic;2(1):18-40.

[14] Behnam N., Hosseini M., Shahbazi S. (2020). A criterion for estimating the minimum drilling mud pressure to prevent shear failure in oil wells. Geotechnical and Geological Engineering;38(1):227-36.

[15] Ezati M., Azizzadeh M., Riahi M. A., Fattahpour V., Honarmand J. (2020). Wellbore stability analysis using integrated geomechanical modeling: a case study from the Sarvak reservoir in one of the SW Iranian oil fields. Arabian Journal of Geosciences;13(4):149.

[16] Allawi R. H., Al-Jawad M. S. (2021). Wellbore instability management using geomechanical modeling and wellbore stability analysis for Zubair shale formation in Southern Iraq. Journal of Petroleum Exploration and Production Technology;11(11):4047-62.

[17] Hoseinpour M., Riahi M. A. (2022). Determination of the mud weight window, optimum drilling trajectory, and wellbore stability using geomechanical parameters in one of the Iranian hydrocarbon reservoirs. Journal of Petroleum Exploration and Production Technology; 12(1):63-82.

[18] Heydari M., Aghakhani Emamqeysi M. R., Sanei M. (2022). Finite element analysis of wellbore stability and optimum drilling direction and applying NYZA method for a safe mud weight window. Journal of Analytical and Numerical Methods in Mining Engineering; 11(29):67-76.

[19] Rezavand, N., Jahani, D., & Asilian, H. (2016). Analysis of Sedimentary Environment and Sequence Stratigraphy of Middle-Late Permian Sediments in Coastal Fars, Iran (Zireh Gas Field, Well ZH-A). *Open Journal of Geology*, *6*(12), 1539.

[20] Fjar E., Holt R. M., Raaen A., Horsrud P. (2008). Petroleum related rock mechanics. Elsevier.

[21] Ameen M. S., Smart B. G., Somerville J. M., Hammilton S., Naji N. A. (2009). Predicting rock mechanical properties of carbonates from wireline logs (A case study: Arab-D reservoir, Ghawar field, Saudi Arabia). Marine and Petroleum Geology;26(4):430-44.

[22] Seyedsajadi S., Aghighi M. A. (2015). Construction and Analysis of a Geomechanical Model for Bangestan Reservoir in Koopal Field. Iranian Journal of Mining Engineering;10(26):21-34.

[23] Asquith G. B., Krygowski D., Gibson C. R. (2004). Basic well log analysis. American Association of Petroleum Geologists Tulsa.

[24] Jaeger J. C., Cook N. G., Zimmerman R. (2009). Fundamentals of rock mechanics. John Wiley & Sons.

[25] Gardner G., Gardner L., Gregory A. (1974). Formation velocity and density—The diagnostic basics for stratigraphic traps. Geophysics;39(6):770-80.

[26] Hottmann C., Johnson R. (1965). Estimation of formation pressures from log-derived shale properties. Journal of Petroleum Technology;17(06):717-22.

[27] Matthews W. (1967). How to predict formation pressure and fracture gradient from electric and sonic logs. Oil and Gas.

[28] Eaton B. A., editor The equation for geopressure prediction from well logs. Fall meeting of the Society of Petroleum Engineers of AIME; 1975: OnePetro.

[29] Zhang J. (2011). Pore pressure prediction from well logs: Methods, modifications, and new approaches. Earth-Science Reviews;108(1-2):50-63.

[30] Azadpour M., Manaman N. S., Kadkhodaie-Ilkhchi A., Sedghipour M.-R. (2015). Pore pressure prediction and modeling using well-logging data in one of the gas fields in south of Iran. Journal of Petroleum Science and Engineering;128:15-23.

[31] Jaeger J., Cook N. (1979). Fundamentals of rock mechanics. Barnes and Noble. Methuen, London, New York, 593p.

[32] Kidambi T., Kumar G. S. (2016). Mechanical earth modeling for a vertical well drilled in a naturally fractured tight carbonate gas reservoir in the Persian Gulf. Journal of Petroleum Science and Engineering;141:38-51.

[33] Zoback M. D. (2010). Reservoir Geomechanics. Cambridge University Press.

[34] Mohr O. (1900). Welche Umstände bedingen die Elastizitätsgrenze und den Bruch eines Materials. Zeitschrift des Vereins Deutscher Ingenieure;46(1524-1530):1572-7.

[35] Mogi K. (1971). Effect of the triaxial stress system on the failure of dolomite and limestone. Tectonophysics;11(2):111-27.

[36] Logan D. L. (2011). A First Course in the Finite Element Method. Cengage Learning.